

Synthetic Biology Toolbox, Including a Single-Plasmid CRISPR-Cas9 System to Biologically Engineer the Electrogenic, Metal-Resistant Bacterium *Cupriavidus metallidurans* CH34

Federico Turco, Marco Garavaglia, Rob Van Houdt, Phil Hill, Frankie J. Rawson, and Katalin Kovacs*

Cite This: <https://doi.org/10.1021/acssynbio.2c00130>

Read Online

ACCESS |



Metrics & More



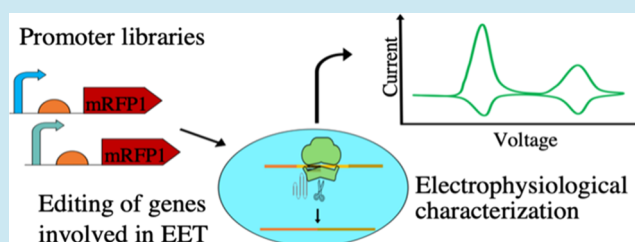
Article Recommendations



Supporting Information

ABSTRACT: *Cupriavidus metallidurans* CH34 exhibits extraordinary metabolic versatility, including chemolithoautotrophic growth; degradation of BTEX (benzene, toluene, ethylbenzene, xylene); high resistance to numerous metals; biomineralization of gold, platinum, silver, and uranium; and accumulation of polyhydroxybutyrate (PHB). These qualities make it a valuable host for biotechnological applications such as bioremediation, bioprocessing, and the generation of bioelectricity in microbial fuel cells (MFCs). However, the lack of genetic tools for strain development and studying its fundamental physiology represents a bottleneck to boosting its commercial applications. In this study, inducible and constitutive promoter libraries were built and characterized, providing the first comprehensive list of biological parts that can be used to regulate protein expression and optimize the CRISPR-Cas9 genome editing tools for this host. A single-plasmid CRISPR-Cas9 system that can be delivered by both conjugation and electroporation was developed, and its efficiency was demonstrated by successfully targeting the *pyrE* locus. The CRISPR-Cas9 system was next used to target candidate genes encoding type IV pili, hypothesized by us to be involved in extracellular electron transfer (EET) in this organism. Single and double deletion strains ($\Delta pilA$, $\Delta pilE$, and $\Delta pilAE$) were successfully generated. Additionally, the CRISPR-Cas9 tool was validated for constructing genomic insertions ($\Delta pilAE::gfp$ and $\Delta pilAE::\lambda_p::gfp$). Finally, as type IV pili are believed to play an important role in extracellular electron transfer to solid surfaces, *C. metallidurans* CH34 $\Delta pilAE$ was further studied by means of cyclic voltammetry using disposable screen-printed carbon electrodes. Under these conditions, we demonstrated that *C. metallidurans* CH34 could generate extracellular currents; however, no difference in the intensity of the current peaks was found in the $\Delta pilAE$ double deletion strain when compared to the wild type. This finding suggests that the deleted type IV pili candidate genes are not involved in extracellular electron transfer under these conditions. Nevertheless, these experiments revealed the presence of different redox centers likely to be involved in both mediated electron transfer (MET) and direct electron transfer (DET), the first interpretation of extracellular electron transfer mechanisms in *C. metallidurans* CH34.

KEYWORDS: *C. metallidurans* CH34, CRISPR, Cas9, direct electron transfer, extracellular electron transfer, genome editing, promoter libraries, riboswitch, mediated electron transfer, microbial fuel cells, type IV pili



INTRODUCTION

Gram-negative *Cupriavidus metallidurans* CH34 displays an extraordinary genomic plasticity¹ that allowed it to evolve a unique combination of metabolic features, such as autotrophic growth on CO₂ as the sole carbon source combined with hydrogenotrophy;^{2,3} degradation of BTEX (benzene, toluene, ethylbenzene, xylene);^{3,4} high resistance to numerous metals;³ biomineralization of gold,⁵ platinum,⁶ silver⁷ and uranium,⁸ and accumulation of polyhydroxybutyrate.⁷ However, despite this exceptional potential as an industrial microbial chassis for applications such as bioremediation, biomining, biosensing, carbon sequestration, and bioprocessing, proof-of-concept studies investigating this microorganism for biotechnological applications are scarce and mostly limited to its use in the bioremediation of metal-contaminated soils⁹ and waters.¹⁰

The major limitations hindering the study and use of *C. metallidurans* CH34 for biotechnological applications are the scarcity of genetic tools that can be adopted by the synthetic biology community to design genetic circuits of predicted outcomes, including the lack of fast marker-less genome editing tools, and of physiological studies unraveling industrially relevant features of *C. metallidurans* CH34 other than those linked to metal resistance. In fact, no genetic part libraries are

Received: March 10, 2022

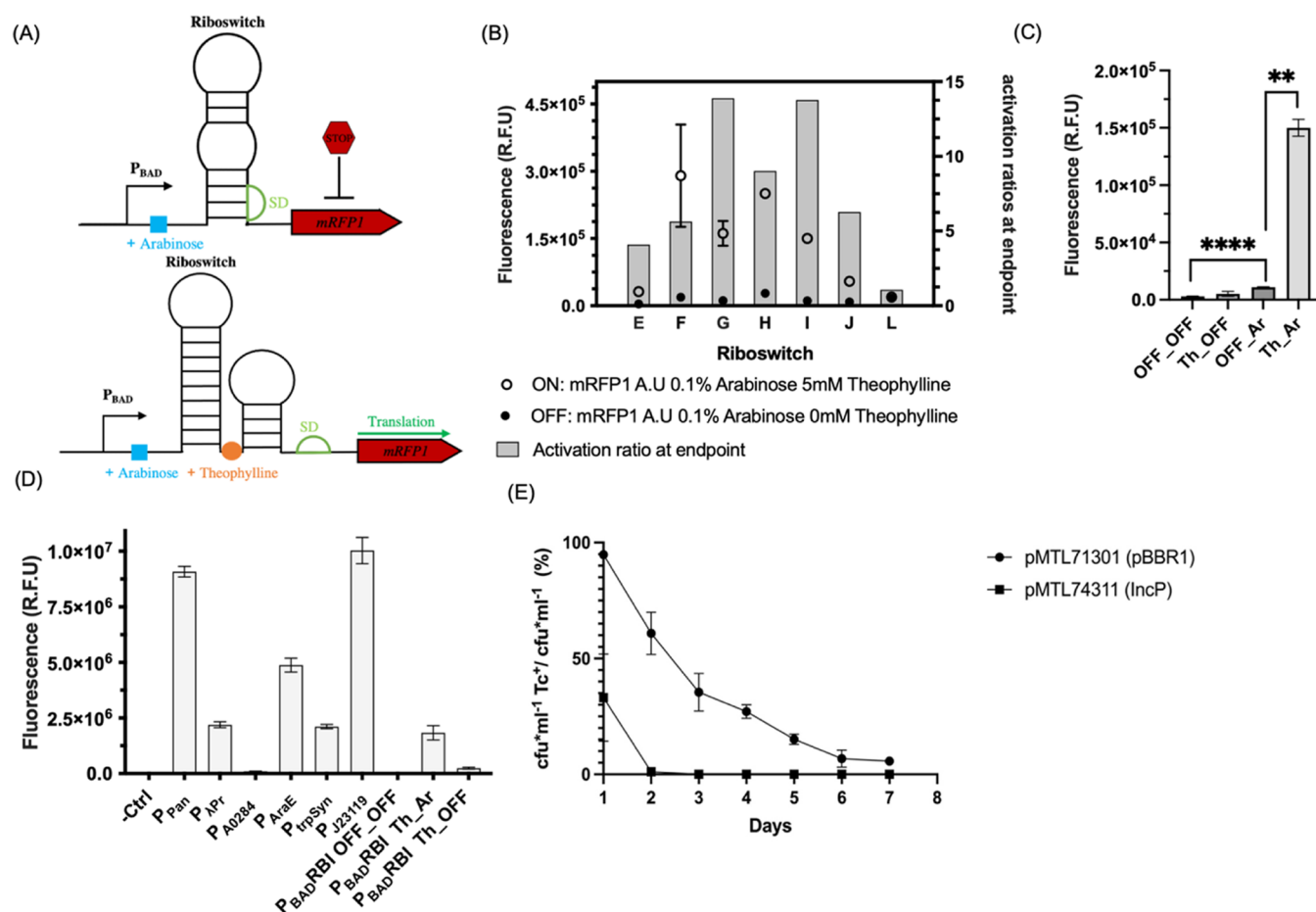


Figure 1. Optimization of the CRISPR-Cas9 system components, promoters, riboswitches, and plasmid backbones. (A) Schematic representation of the dual controlling mechanism using the arabinose inducible promoter (P_{BAD} ; transcriptional control) cloned upstream of a riboswitch library in the absence and presence of theophylline, a translational regulator that controls the translation of a modified red fluorescent protein (mRFP1, red). In the presence of arabinose and in the absence of theophylline, the SD (green) is not accessible for the translation of the mRFP1. The addition of theophylline (bottom panel, orange) results in the conformational change of the mRNA, making the SD available for mRFP1 translation. (B) Normalized activity of the P_{BAD} -driven and theophylline-controlled riboswitch library (six riboswitch sequences labeled as E, F, G, H, I, J as previously described^{23,38} and L, control without a riboswitch sequence) cloned upstream the mRFP1 fluorescent protein. Fluorescence was measured in relative fluorescence units (RFU). The mRFP1 translation levels were measured in both the ON state (0.1% L-arabinose and 5 mM theophylline) and in the OFF state (0.1% L-arabinose only), and these are represented by empty and filled circles, respectively. The activation ratio (fluorescence difference between the ON and OFF states) at the endpoint is represented by gray bars. (C) Relative contribution of the RBI (riboswitch "I", best performing as seen in (B)) in translational repression of the mRFP1 measured in RFU. The OFF_OFF state represents the RFU measured in the absence of both arabinose and theophylline (very low level of transcription and translation), the Th_OFF state represents the RFU measured in the absence of arabinose and the presence of theophylline, the OFF_Ar represents the RFU measured in the presence of arabinose and the absence of theophylline, while the Th_Ar represents the RFU measured in the presence of both arabinose and theophylline. (D) Normalized fluorescence of the mRFP1 fluorescent protein in *C. metallidurans* CH34 transformed with a multicopy plasmid (pMTL71301) carrying the mRFP1 cloned downstream of a constitutive promoter library (six promoter sequences labeled as P_{Pan} , P_{Apt} , P_{A0284} , P_{AraE} , P_{TtpSyn} , P_{J23119}), measured alongside a negative control (–Ctrl, mRFP1 without a promoter sequence) and the previously characterized RBI (as seen in (C)). (E) Plasmid stability test of two replicative plasmids pMTL71301, carrying the pBBR1 origin of replication and pMTL74311 carrying the IncP origin of replication in *C. metallidurans* CH34. Both plasmids carry the tetracycline resistance gene, and the plasmid loss was determined after 1–7, 24 h serial passages in media without selection and as the ratio of colony forming units (cfu) after replica plating on agar plates with ($\text{cfu}\cdot\text{mL}^{-1}\text{Tc}^+$) and without ($\text{cfu}\cdot\text{mL}^{-1}$) tetracycline, as described previously.⁴² Error bars represent standard deviation ($n = 4$), and statistical significance was calculated by means of the Mann–Whitney test (** $p < 0.00001$, *** $p < 0.001$).

currently available for *C. metallidurans* CH34. As such, developing and tailoring synthetic genetic circuits are difficult as knowledge of functional inducible and constitutive promoters with a diverse range of activity is lacking. Furthermore, genome editing in *C. metallidurans* CH34 has historically been performed by means of suicide plasmid-based allelic exchange technologies¹¹ bolstered by counterselection and the transient expression of the *cre* recombinase to excise the antibiotic cassette.^{11,12} However, this process depends on multiple conjugation steps, which is not only a long and tedious process

(e.g., when compared to electroporation¹³) but can also activate endogenous mobile genetic elements, leading to unwanted off-target modifications.¹⁴

Since their discovery, spCas9 systems have been extensively exploited as efficient and robust tools for the construction of recombinant prokaryotic¹⁵ and eukaryotic strains.^{15,16} Development of successful CRISPR-spCas9 technologies for selection of HR-mediated recombinant isolates in *Corynebacterium glutamicum*,¹⁷ *Rhodobacter sphaeroides*,¹⁸ *Methylococcus capsulatus*,¹⁹ *Cupriavidus necator* H16,²⁰ and *Clostridia* sp.²¹²¹ was shown to

be dependent on two main factors. On the one hand, Cas9 expression needs to be tightly controlled via the use of inducible promoters²⁰ and/or orthogonal synthetic riboswitches²¹ to prevent its toxicity. On the other hand, the use of strong constitutive promoters for the expression of single guide RNA (sgRNA) is required. However, as different microbes respond dramatically differently to regulatory sequences, host-dependent optimization of CRISPR-Cas systems is a prerequisite for their successful application.

The most recent proof-of-concept study focusing on potential biotechnological applications of *C. metallidurans* CH34 highlighted its capacity to degrade toluene while generating bioelectricity in microbial fuel cells (MFCs),²² thereby opening the possibility to use this microorganism for the remediation of wastewaters contaminated with recalcitrant xenobiotic and simultaneous recovery of energy. As current wastewater treatment technologies require more than 2% of the world's electricity production (with local municipalities using up to 20% of their energy supply for recovery of wastewaters),²³ development of efficient MFC technologies able to purify wastewaters and recover energy in the form of electricity is needed. Nevertheless, MFCs struggle to find commercial applications due to a low voltage output.²⁴ To circumvent this issue, synthetic biology toolboxes, which encompass promoter libraries and CRISPR-Cas technologies, can be exploited to precisely tune and control extracellular electron transfer (EET) pathways, enhance the electron transfer rate between the electrode and the bacteria, and unravel EET mechanisms in different bacteria.²⁵

The study of bacterial EET has been mainly focused on *Shewanella* spp.²⁶ and *Geobacter sulfureducens*,²⁷ two electroactive bacteria archetypical for mediated and direct external electron transfer, respectively. Of particular interest are the type IV conductive pili of *G. sulfureducens*,²⁷ which are polymers of the PilA protein²⁸ and have been postulated to be essential for the high anodic current generation in MFC with pure cultures of *G. sulfureducens*.²⁹ PilA-based nanowires are therefore a promising sustainable conductive material that can be produced without the use of harsh chemicals while recovering energy and purifying wastewaters.³⁰ In 2013, it was discovered that during the process of gold biomineralization, *C. metallidurans* CH34 formed biofilms on gold granules. Cells in the biofilm were shown to produce proteinaceous structures, which were hypothesized to be conductive nanowires used by the bacteria to “breathe” excess electrons outside the cell,³¹ thereby possibly expanding the list of bacteria employing type IV pili for EET.

In this study, we developed *C. metallidurans* CH34 as an industrial microbial chassis by (i) constructing a toolbox with constitutive and tightly controlled promoters, (ii) developing a single-plasmid CRISPR-Cas9 system deliverable by electroporation for marker-less editing and chromosomal DNA insertions, and (iii) demonstrating the use of this CRISPR-Cas9 system by exploring the involvement of the type IV pili in EET.

RESULTS AND DISCUSSION

Optimization of Cas9 and sgRNA Transcription and the Design of the Single-Plasmid Genome Editing System. To successfully implement the CRISPR-Cas9 system for engineering *C. metallidurans* CH34, we aimed at (i) the transient expression and tight regulation of the toxic Cas9 protein, (ii) a high constitutive expression of the sgRNA, and (iii) the integration of the regulatory elements, the Cas9 coding

sequence, a sgRNA and homologous template in an easy-to-cure plasmid platform.

First, to achieve tightly regulated and transient expression of *cas9*, a two-level system was constructed based on the L-arabinose-inducible P_{BAD} promoter and a theophylline-dependent riboswitch library. These riboswitches were composed of a linker sequence, an aptamer domain specific for theophylline, and an expression domain harboring the Shine Dalgarno sequence (SD).³² When theophylline is absent from the growth media, the SD is occluded in the secondary structure formed by the transcribed riboswitch nucleotide sequence. However, upon ligation of theophylline to the aptamer domain, relaxation of the secondary structure occurs, and the SD becomes available for translation (Figure 1A). Theophylline-dependent riboswitches were previously successfully employed by Cañadas et al. for the controlled expression of *cas9* in *Clostridia* species.²¹ Here, we placed the P_{BAD} promoter upstream of the theophylline-dependent riboswitches F–J³² and E²¹ used by Cañadas and colleagues. A construct lacking any riboswitch (L, Linker) but maintaining the SD was used as a control. The plasmid series pMTL71301_P_{BAD}_RBX_mRFP1 (where “X” represents the riboswitch under investigation) was transformed into *C. metallidurans* CH34 and mRFP1 expression scored by fluorescence intensity (au) (Table S8). The P_{BAD}-riboswitch library was also tested in the presence of L-arabinose only (OFF state) to provide information regarding the ability of the riboswitch alone to control expression at the posttranscriptional level and in the presence of both L-arabinose and theophylline (ON state). The P_{BAD}_RBE, P_{BAD}_RBG, P_{BAD}_RBI, and P_{BAD}_RBJ constructs exhibited good repression of mRFP1 expression in the OFF state. However, P_{BAD}_RBE and P_{BAD}_RBJ were excluded from further consideration because they showed a low activation ratio, which is not ideal since suboptimal Cas9 expression levels may result in an inefficient selection of recombinant isolates.³³ P_{BAD}_RBF was also excluded because of its high variability in terms of maximal mRFP1 expression levels recorded in the ON state (Figure 1B). Next, the relative contribution of the P_{BAD} and RBI elements was further investigated. The P_{BAD}_RBI system without both inducers (OFF_OFF) showed negligible mRFP1 expression. The addition of theophylline alone (Th_OFF) resulted in a small increase in expression (not statistically significant), which could be attributed to the background leakiness of the P_{BAD} promoter.³⁴ However, while addition of only L-arabinose (OFF_Ara) resulted in a small but significant increase in mRFP1 production (Mann–Whitney test, $p < 0.00001$), the difference in mRFP1 expression between the OFF_Ara and Th_Ara states (with both inducers) was much more pronounced (Mann–Whitney test, $p < 0.001$), suggesting that the riboswitch effectively prevented translation by occluding the SD (Figure 1C). These results strongly indicate that the P_{BAD}_RBI combination could be used as a reliable ON/OFF system to ensure tight regulation of Cas9 levels.

To achieve a high constitutive expression of sgRNA in the CRISPR-Cas9 system, the P_{PanJ},³⁵ λ_{P_{trp}},³⁶ P_{A0284},³⁷ P_{AraE},²¹ P_{J23119}, and P_{trp_{syn}}^{38,38} constitutive promoters were cloned upstream of *mRFP1*, thereby generating the plasmid series pMTL71301_X_mRFP1 where “X” stands for the specific constitutive promoter under study (Table S8). The plasmid series was transformed into *C. metallidurans* CH34 and mRFP1 expression scored by fluorescence intensity (au) (Figure 1D). While some promoters showed low to medium activity, P_{Pan} and P_{J23119} displayed strong constitutive expression (Figure 1D).

P_{J23119} is a synthetic, fully characterized promoter of only 35 bp and much shorter than P_{Pan} (400 bp); therefore, it was selected for further work as it can more easily be cloned by designing primers with the promoter sequence as a spacer region (Table S9).

Since molecular tools for *C. metallidurans* CH34 are still very limited, the screening of constitutive and double inducible promoter libraries provides valuable information for the scientific community interested in using this species for biotechnological and synthetic biology applications. Promoters with low activities are useful for complementation studies (e.g., for auxotrophy)³⁹ or the expression of toxic or difficult-to-purify proteins, i.e., to avoid the formation of inclusion bodies and improve the fraction of soluble protein.⁴⁰ Moreover, leaking expression of a recombinant protein often leads to toxicity, growth deficiency, cell death, and loss of product. To this extent, dual expression control systems have been proposed as an efficient tool to suppress the leaky expression of proteins.⁴¹

Third, to find an easily curable plasmid as a backbone for the CRISPR-Cas9 system, a plasmid stability test using plasmid pMTL71301 (pBBR1 replication origin) and pMTL74311⁴² (IncP replication origin with single point mutation R271C in the *trfA* gene conferring high copy number⁴³) was performed in *C. metallidurans* CH34, as previously described by Ehsaan et al.⁴² Plasmid pMTL74311 was completely lost after 48 h of continuous culture in the absence of selection, while plasmid pMTL71301 was still detectable in the cultures after 7 days (Figure 1E). For this reason, pMTL74311 was chosen as a suitable vector for the CRISPR-Cas9 system. In *C. necator* H16, the copy numbers per cell of pBBR1 and pCM271 (IncP *ori* with the R271C point mutation in *trfA*) were reported to be ~40 for both replicons.⁴² Therefore, mRFP1 expression levels from plasmid pMTL74311 were assumed to be comparable to those quantified with the promoter libraries cloned in pBBR1 derivatives. A rapidly curable plasmid accelerates the isolation of plasmid-less mutant clones significantly.⁴⁴ An alternative approach is the use of a temperature-sensitive plasmid backbone to achieve conditional plasmid propagation.⁴⁵ However, such replicons cannot be used in *C. metallidurans* as it displays an aberrant phenotype at temperatures of 37–42 °C, which are required to induce plasmid loss.³

Validation of the CRISPR-Cas9 System. Based on the data above, a CRISPR-Cas9 system was constructed based on the pMTL74311 (IncP) backbone with $P_{BAD_RBI-cas9}$ and the $J23119$ promoter driving expression of the sgRNA. To assess if this CRISPR-Cas9 system was functional, we first constructed it with *pyrE*-specific sgRNA and HR arms to obtain a marker-free *pyrE* knockout in *C. metallidurans* CH34. The *pyrE* gene was selected as a target for the first evaluation because of the simplicity of screening for the $\Delta pyrE$ phenotype. Replica plating of bacterial colonies on minimal media agar plates with or without uracil can be used to quickly select for uracil auxotrophs, thereby allowing identification of recombinant clones, even in the case of low selection efficiency of Cas9. Replica plating of *C. metallidurans* CH34 isolates that appeared after theophylline and arabinose induction showed the successful isolation of recombinant mutants (Figure 2B shows a representative replica plating experiment). Randomly selected colonies screened by colony PCR and further confirmed via Sanger sequencing corroborated the successful isolation of *pyrE* knockouts, although recombination efficiency varied between each mother colony (MC) (Figure 2C,D). The overall efficiency of $\Delta pyrE$ mutant isolation was $60 \pm 14.7\%$ ($n = 4$, standard deviation),

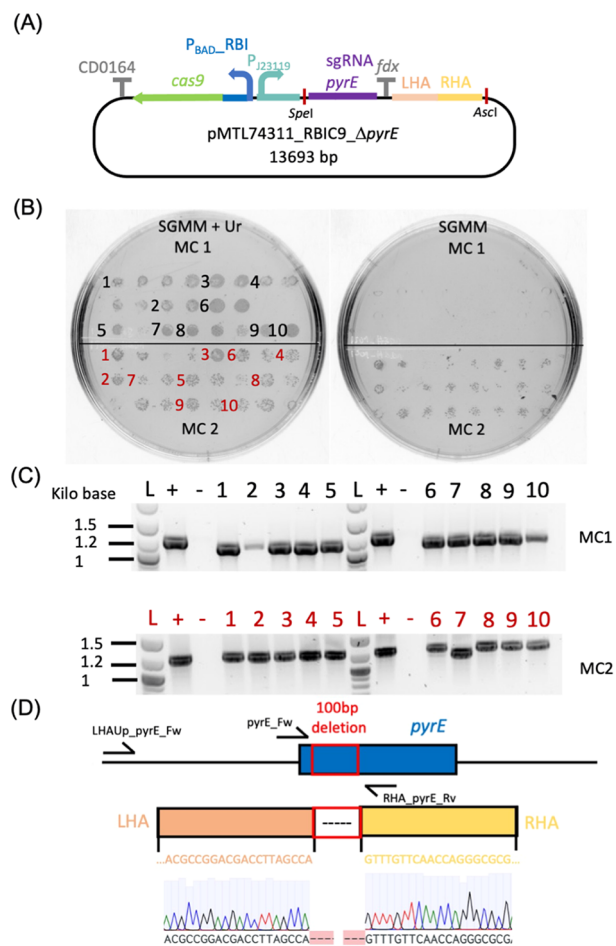


Figure 2. Isolation of *C. metallidurans* CH34 $\Delta pyrE$ deletion mutants using the optimized CRISPR-Cas9 system. (A) Graphical representation of the pMTL74311_ $P_{BAD_RBI}cas9_{\Delta pyrE}$ plasmid (13 693 kb) used to generate the *pyrE* deletion mutants. This plasmid carries two back-to-back transcriptional units and the homology regions (left homology Arm-LHA and right homology Arm-RHA) for homologous recombination. The first transcriptional unit is the *cas9* driven by the P_{BAD} promoter and translationally regulated by the *RBI* riboswitch, terminated by the CD164 terminator sequence, the second is the small guide RNA (sgRNA) targeted to the *pyrE* region driven by the strong, constitutive, synthetic promoter P_{J23119} , terminated by the ferredoxin (*fdx*) terminator sequence. The restriction sites *SpeI* and *AscI* are highlighted. These can be used to modify the CRISPR plasmid for targeting the desired sequence. (B) Replica plating of two mother colonies (MC1 and MC2) on SGMM (sodium gluconate minimal medium) agar plates supplemented with uracil (+ Ur, left panel) or without uracil (right panels). Isolates selected for the following colony PCR are labeled in black and red for MC1 and MC2, respectively. (C) Agarose gel of amplicons obtained by PCR with primer pairs LHAUp_pyrE_Fw (binding outside the LHA)/pyrE_Rv on *C. metallidurans* CH34 colonies growing on SGMM agar plates. The expected amplicon sizes were ~1.2 and 1.1 kb for the wild type and $\Delta pyrE$ knockout, respectively. For each gel, L, +, and – lanes were loaded with a DNA ladder and PCR products of the positive control (PCR amplicons from *C. metallidurans* CH34) and the negative control (PCR amplicon of pMTL74311_ $P_{BAD_RBI}cas9_{\Delta pyrE}$), respectively. (D) Schematic representation of the *pyrE* locus reporting the *pyrE* gene (blue), the target deletion (red box), and the left and right homology arms (light orange and yellow, respectively) with the respective nucleotide sequences. The Sanger sequencing chromatogram of one of the isolates is also reported. Primer pyrE_Fw was used for sequencing the selected colonies.

with selection efficiencies varying greatly between each experiment and each mother colony induced (Table 1). The

Table 1. Summary of the *pyrE* Knockout Experiment^a

target	exp. number	MC ID	mutants/isolates screened	selection efficiency (%)	overall efficiency (%)
<i>pyrE</i>	1	1	12/12	54	60 ± 14.7
		2	1/12		
	2	3	12/12	100	
		4			
	3	5	2/12	58	
		6	12/12		
	4	7	3/12	29.1	
		8	4/12		

^aReported error represent standard deviation ($n = 4$, error is reported as the standard deviation).

evolution of bacterial cells is well known to cause the loss of performance in genetically modified bacterial strains due to mutation of recombinant DNA sequences,⁴⁶ suggesting that “escapees” might be able to circumvent Cas9 selection, putatively by inactivating the portion of the *cas9* gene coding for its endonuclease domain or the promoter sequences controlling expression of *cas9* or the sgRNA. Nevertheless, the one mother colony that failed to produce knockouts did not show any growth on induction plates (MC3 from experiment number 2), suggesting that Cas9 selection may be, in some cases, 100% efficient in preventing the growth of nonrecombinant clones.

Next, we targeted genes hypothesized to be involved in EET in *C. metallidurans* CH34. A bioinformatics analysis was carried out with the Uniprot BLAST tool to identify *G. sulfureducens* PilA (GSU1496) homologs in the proteome of *C. metallidurans* CH34. We found that in *C. metallidurans* CH34, Rmet_0472 and Rmet_0473 (annotated as type IVa pili PilA and PilE, respectively) were 49.1 and 42.4% identical to the full length of *G. sulfureducens* PilA. Moreover, in *G. sulfureducens*, GSU1496 and GSU1497 are found adjacent (similarly to *C. metallidurans* CH34) and functionally related to each other.⁴⁷ Both GSU1496 and GSU1497 were found to be upregulated when *G. sulfureducens* was grown in MFC, and the GSU1497 knockout strain was also discovered to have the impaired capability of producing anodic currents.⁴⁷ Therefore, given the genomic arrangement of Rmet_0472/Rmet_0473, the similarity of both genes with GSU1496 (Figure S1), the need for both GSU1496 and GSU1497, as well as the identical mapped peptidase cleavage site (G29) between Rmet_0472 and GSU1496, we hypothesized Rmet_0472 and Rmet_0473 to be involved in EET in *C. metallidurans* CH34. To test our hypothesis, plasmids pMTL74311_RBIC9_Δ*pilA*, pMTL74311_RBIC9_Δ*pilE*, and pMTL74311_RBIC9_Δ*pilAE* were constructed to generate knockouts of *pilA*, *pilE*, and *pilAE*, respectively. Plasmids pMTL74311_RBIC9_Δ*pilAE*::*gfp* (*gfp* expression controlled by a native promoter) and pMTL74311_RBIC9_Δ*pilAE*:: λ_{pr} *gfp* (*gfp* expression controlled by a constitutive λ_{pr} promoter) were also created to determine the ability of the CRISPR-Cas9 system to perform insertions, a necessary feature to develop recombinant strains for metabolic engineering. Plasmid pMTL74311_RBIC9_Δ*pilAE* was then delivered to *C. metallidurans* CH34 via conjugation. The MCs induced to target the *pilAE* locus resulted in a 100% editing efficiency. However, recombination of isolates from induction of MC2 resulted in the

deletion of about 300 bp in the LHA (Figure S2 and Table S3). Electroporation was also investigated for plasmid delivery as conjugation has been reported to induce the SOS response genes, which could trigger DNA recombination,⁴⁸ thereby reducing the chances of obtaining isogenic mutants. Electroporation would also save a considerable amount of time (~2 days), particularly when employing a quick protocol for the preparation of electrocompetent cells. Furthermore, conjugation can also trigger endogenous mobile genetic elements creating unwanted off-target modifications.⁴⁹ When plasmids were delivered by electroporation to target the *pilA* and *pilE* loci, the efficiency of selection was 12.5% for both targets. Genomic integration of the *gfp* gene with the concomitant deletion of the *pilAE* operon was also successfully achieved with an overall efficiency of 50%. However, no GFP expression was detected using super-resolution confocal microscopy. In *Pseudomonas aeruginosa*, the presence of the PilA protein was suggested to be required for its own regulation as a complex interaction between the PilSA two-component system results in the autoregulation of *pilA* expression.⁵⁰ Thereby, it is possible that a similar regulation of the expression of the *pilA/E* genes may also occur in *C. metallidurans* CH34 and thus the deletion of the *pilAE* locus may have impaired expression from their native promoter, resulting in no production of GFP.

Next, the insertion of *gfp* under control of the constitutive λ_{pr} promoter was tested. Electroporation of plasmid pMTL74311_P_{BAD}RBIC9_Δ*pilAE*:: λ_{pr} *GFP* resulted in low transformation efficiency. Moreover, only 4 out of the 10 induced mother colonies produced clones on LB IND plates, none of which carried the desired mutation. The same plasmid was also delivered by conjugation, with an ~100-fold increase in transformation efficiency (Figure S4). Two mother colonies were induced, and a total of 2 out of 93 isolates were confirmed by cPCR (colony PCR) to be Δ*pilAE*:: λ_{pr} *GFP* mutants (2.03% efficiency). Therefore, although electroporation can be used, conjugation may improve editing efficiency for more difficult targets (e.g., for the integration of CDSs coding toxic proteins or in case of low electroporation efficiency). *C. metallidurans* CH34 Δ*pilAE*:: λ_{pr} *GFP* was visualized under structural illumination microscopy. The wild-type strain was used to measure basal fluorescence levels, which were used as a reference for comparison with *C. metallidurans* CH34 Δ*pilAE*:: λ_{pr} *GFP* (Figure 3). All knockouts were confirmed and successfully cured of the editing CRISPR-Cas9 plasmid by overnight growth in nonselective media followed by replica plating and cPCR with primers amplifying *cas9*. Finally, whole-genome sequencing of the knockout strains showed that only one of the mutants carried off-target mutations (Table S5). Results of the validation knockout experiments in terms of Cas9-mediated selection efficiencies are presented in Table 2, while representative agarose gel electrophoresis pictures of the cPCR products confirming *pilE* and *pilA*, *pilAE*::*GFP*, and *pilAE*:: λ_{pr} *GFP* knockouts are reported in Figure S2.

Use of Cyclic Voltammetry to Study the Involvement of Type IV Pili in EET of a *C. metallidurans* CH34 Biofilm on Screen-Printed Carbon Electrodes. To confirm the successful colonization of the screen-printed carbon electrodes (SPCEs) by *C. metallidurans* CH34, these were subjected to live/dead staining after each cyclic voltammetry experiment and imaged using confocal microscopy. Bare electrodes incubated in the absence of bacterial cultures were used as a negative control in these experiments. Horizontal sections and Z-stacks of the biofilm-colonized electrodes showed the successful formation of

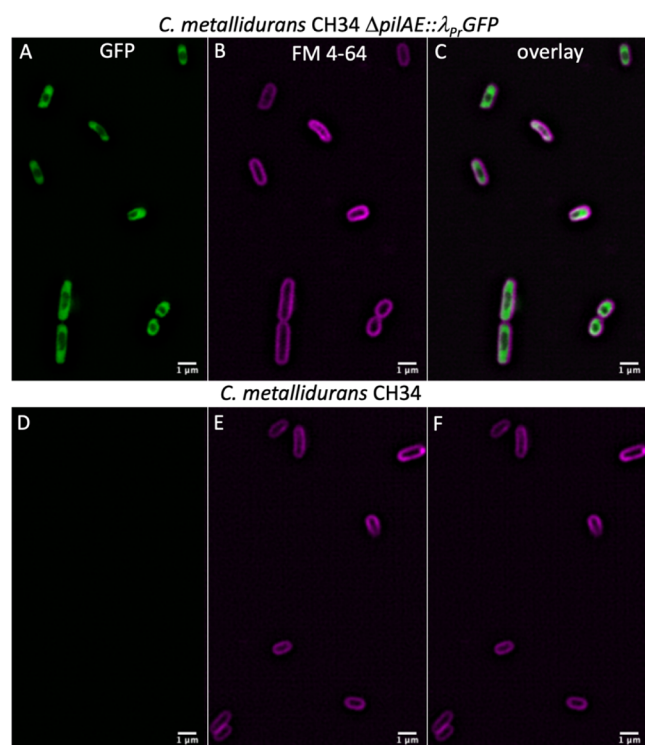


Figure 3. Localization of constitutively expressed GFP protein integrated into the genome of *C. metallidurans* by structural illumination microscopy (SIM). Panels (A)–(C) represent images of *C. metallidurans* CH34 $\Delta pilAE::\lambda_{pr},GFP$ expressing GFP intracellularly (A, bandpass filters BP 495–550 + LP 750), the cell membrane stained with FM-64 FX membrane dye (B, bandpass filter LP 655), and the overlaid channels (C). Panels (D)–(F) represent the wild-type *C. metallidurans* CH34 control strain, imaged under the same conditions as above.

Table 2. Summary of the Validation Experiment of the CRISPR-Cas9 System

target	delivery	mutants/screened	selection efficiency* (%)
<i>pilAE</i>	conjugation	16/16	100
<i>pilA</i>	electroporation	3/24	12.5
<i>pilE</i>	electroporation	3/24	12.5
<i>pilAE::GFP</i>	electroporation	12/24	50
<i>pilAE::λ_{pr},GFP</i>	electroporation	0/24	0
<i>pilAE::λ_{pr},GFP</i>	conjugation	2/93	2.04

a biofilm monolayer with most of the cells being alive, indicating that current peaks in the biofilm-modified electrodes resulted from the electroactivity of *C. metallidurans* CH34 (Figure S6). Cyclic voltammograms of the biofilm-coated SPCEs and negative controls were recorded at 20 mV/s. The biofilm-coated SPCEs showed a cathodic (reduction) and an anodic (oxidative) peak at ~ 0 and 0.3 V. The negative control showed two smaller redox peaks at -0.1 V (reduction) and 0.1 V (oxidation) (Figure 4A left and mid panels represent the voltammograms as recorded and the same curves after baseline subtraction, respectively, between -0.4 and 0.4 V). The current peaks observed in the biofilm-modified SPCE were significantly higher than in the negative control (Mann–Whitney test $n = 4$, $p < 0.05$), thereby confirming the presence of redox centers involved in EET in *C. metallidurans* CH34 (Figure 4A, right panel). Next, to characterize the electron transfer behavior

further, a scan rate experiment was performed. The redox couple observed at 20 mV/s could be observed at all scan rates for the biofilm-coated SPCEs, but not for the negative control (Figure 4B left and mid panels, respectively). The linear relationship between the cathodic peak and the square root of the scan rate suggested a diffusion-controlled EET system (Figure 4B, right panel). However, the anodic current peaks showed no linear relationship with either the scan rate or its square root and displayed reduced intensity when compared to the cathodic current peak (Figure 4B right panel and Figure S7 top panel). Furthermore, shifting of the cathodic and anodic peaks toward more negative and positive potentials, respectively, was also observed (Figure S7 bottom panel), which was previously reported to be due to a sluggish charge transfer rate and solution resistance.⁵¹ These observations suggested that the observed phenomenon was of quasi reversible ErCi (reversible electron transfer followed by an irreversible homogeneous chemical reaction) of diffusive nature.⁵² Cyclic voltammetry experiments of *G. sulfureducens* in MFC under acetate-oxidizing conditions showed anodic currents arising from surface-adsorbed and diffusion-limited mechanisms at different scan rate regimes. This complex interaction resulting in a “bimodal behavior” was discussed to be due to redox molecules confined in the biofilm.⁵³ This electrochemical response is typical of well-established and thick biofilms of *Geobacter* and shows similarities to the catalytic response of glucose oxidase enzymes trapped in a redox conductive epoxy cement, which displays symmetric redox current peaks at slow scan rates typical of adsorbed species but exhibits classic diffusion-limited behavior at high scan rates.⁵⁴ However, the *C. metallidurans* CH34 biofilm showed the presence of a monolayer of cells (z-stack Figure S7), excluding the complex interplay of redox molecules trapped in thick biofilms and limiting data interpretation to the presence of soluble redox mediators of an ErCi system.

Next, to resolve potential redox peaks with low electrochemical activity, CV experiments were repeated at 1 mV/s. Two redox couples (redox¹ and redox²) were observed (Figure 5A, left and mid panels represent the voltammogram as recorded and the same curves after baseline subtraction, respectively) with peak potentials of 0.3 and -0.16 V, respectively, which could not be observed in the negative control (Figure 5A, right panel). Both centers showed no peak separation and a ratio $I_{Rd}/I_{Ox} \neq 1$, thereby indicating two electrochemically active species adsorbed on the electrode surface to be responsible for EET in *C. metallidurans* CH34. To study the putative involvement of type IV pili in the EET process, *C. metallidurans* CH34 $\Delta pilAE$ was studied by CV at 1 mV/s. Neither differences in the shape of the voltammogram nor in the current intensity were observed between the parental strain and the $\Delta pilAE$ mutant, indicating that type IV pili are not involved in EET under the conditions tested (Figure 5B left and right panels, respectively). This null finding is important as the variables studied in this work inform on the role of electron transfer via conductive pili in *C. metallidurans* CH34, which has not been observed before but has only been hypothesized in a previous publication.³¹ Altogether, these results showed that *C. metallidurans* CH34 is capable of EET by means, possibly in a similar fashion to *Shewanella* MR1, which uses a set of periplasmic⁵⁵ and outer membrane⁵⁶ cytochromes and soluble electron carriers⁵⁷ for electron storage and release to terminal electron acceptors.⁵⁸

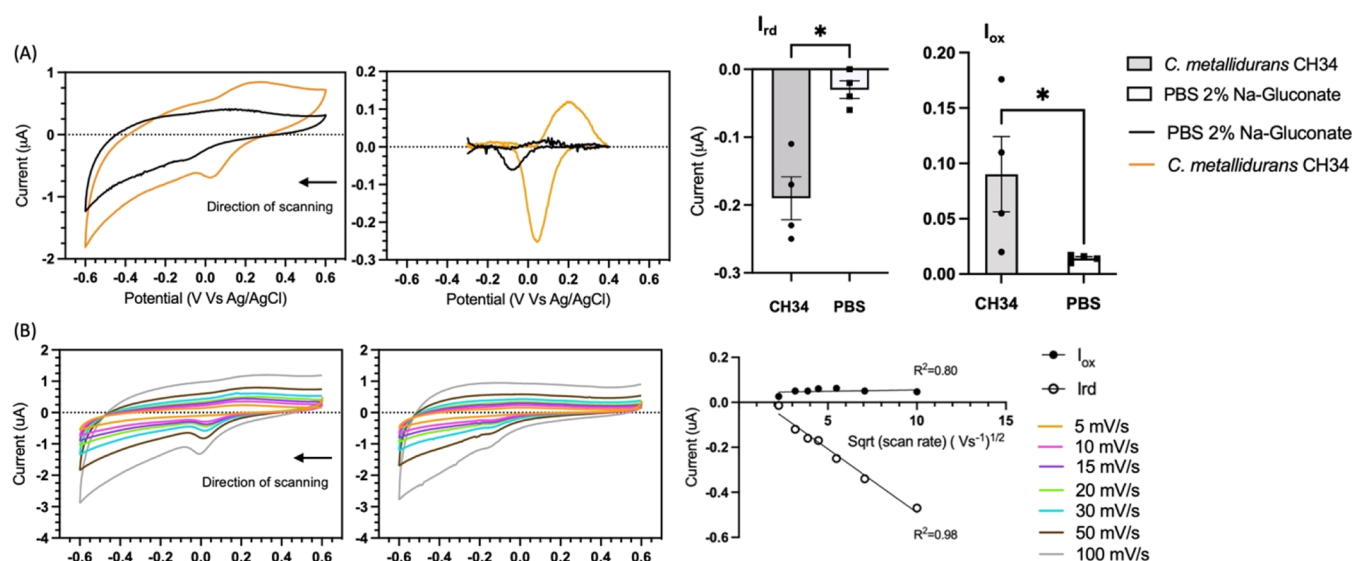


Figure 4. Cyclic voltammetry experiments of *C. metallidurans* CH34 grown on SPCEs and negative control. (A) Cyclic voltammetry at 20 mV/s. From left to right: (i) graph showing representative cyclic voltammograms of the biofilm-coated SPCE (orange voltammograms) and negative control (black voltammograms), (ii) voltammograms after baseline subtraction, and (iii) bar diagrams of the reduction and oxidation current peaks (I_{rd} and I_{ox} , respectively) of the SPCE modified with *C. metallidurans* CH34 (gray bars) and negative control (white bars) are shown from left to right. (B) Scan rate experiment between 5 and 100 mV/s. From left to right: (i) graphs of the scan rate experiments of the biofilm-coated SPCE, (ii) negative control, and (iii) plot of the peak currents against the square root of the scan rate are reported, respectively, from left to right. Error bars represent the standard deviation ($n = 4$), and statistical significance was calculated by means of the Mann–Whitney test ($*p < 0.05$).

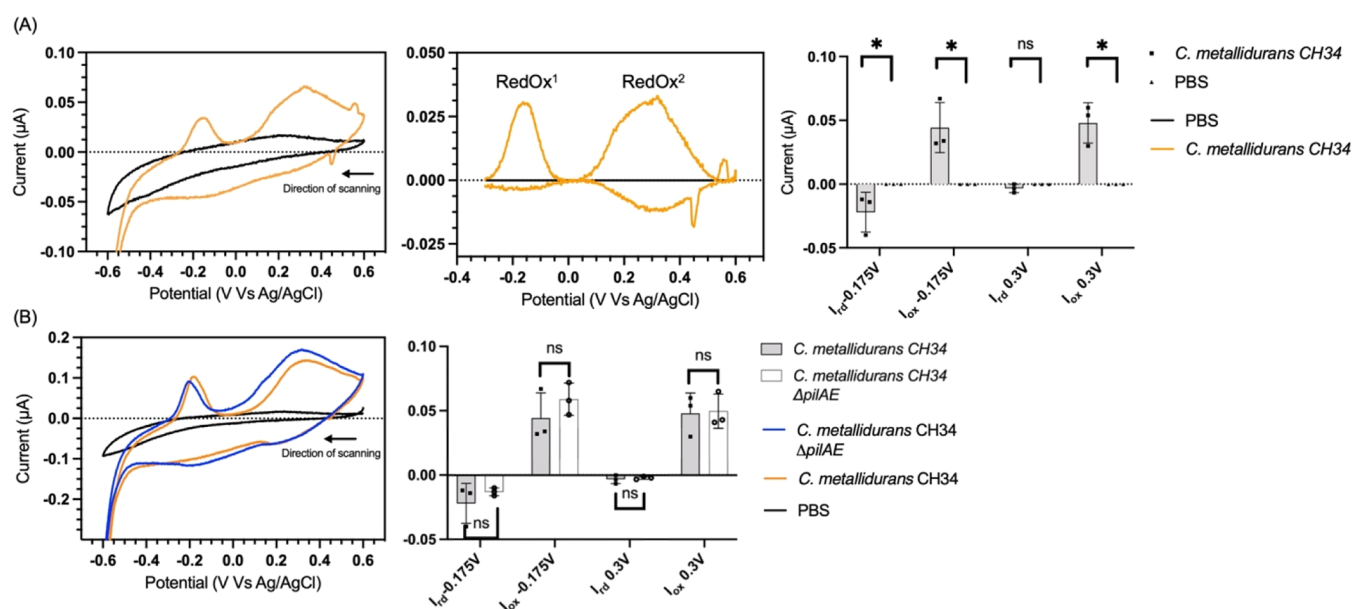


Figure 5. Cyclic voltammetry experiments at 1 mV/s of *C. metallidurans* CH34 and *C. metallidurans* CH34 $\Delta pilAE$ biofilms on SPCEs. (A) Cyclic voltammetry experiments of the SPCE modified with biofilms of *C. metallidurans* CH34 (orange tracks) and SPCE negative control (black tracks). From left to right: (i) panel of a representative voltammogram, (ii) current peaks after baseline subtraction, and (iii) bar diagrams of the current peaks of redox¹ and redox² are reported, respectively, from left to right. (B) Cyclic voltammetry experiment of the SPCE modified with biofilms of *C. metallidurans* CH34 (orange), *C. metallidurans* CH34 $\Delta pilAE$ (blue), and SPCE incubated without the cell cultures (black tracks). The left panel shows a representative voltammogram. The right panel displays a bar diagram of the oxidation and reduction current peaks of *C. metallidurans* CH34 and *C. metallidurans* $\Delta pilAE$. Error bars represent the standard deviation ($n = 3$), and statistical significance was calculated by means of the Mann–Whitney test ($*p < 0.05$).

CONCLUSIONS

In this study, a CRISPR–Cas9 tool for genome editing of *C. metallidurans* CH34 was developed. Preliminary steps included optimizing the expression level of the sgRNA and Cas9, pivotal to minimizing the toxicity of Cas9 and improving the overall efficiency of the system. Constitutive promoters with a wide

range of activity and a hybrid ON/OFF system composed of the inducible P_{BAD} and ncRNAs riboswitches for complete repression of expression in the absence of the inducers were characterized and optimized. This is the first comprehensive library of constitutive and inducible regulative elements for *C. metallidurans* CH34, applicable much broader than the scope of

this work. Our developed CRISPR-Cas9 system showed to be robust with an isolation efficiency of recombinant clones ranging between 2 and 100%.

In addition, the time-honored electrochemistry of cyclic voltammetry was applied to examine electron exchange mechanisms between the electrode surface and *C. metallidurans* biofilms. A comparison of the *C. metallidurans* CH34 parental and $\Delta pilAE$ strain did not show evidence of the involvement of type IV pili in the transfer of electrons under the conditions tested. Nevertheless, it did reveal the presence of different redox centers likely to be involved in both MET and DET. Two of these centers are likely to be outer membrane cytochromes forming direct contact between the cell and the electrode surface or polymers involved in electron storage and release. These data represent a first suggestion of the mechanisms *C. metallidurans* CH34 uses for extracellular electron transfer and shed light on the intricate multicomponent systems likely to be composed of cytochromes and diffusive mediators, which carry out oxidation and reduction under the limitation of a carbon source and a terminal electron acceptor.⁵⁹

MATERIALS AND METHODS

Bacterial Strains and General Growth Conditions. The general growth of *C. metallidurans* CH34 and derivative strains was performed in a lysogeny broth (LB) at 30 °C. *Escherichia coli* was grown in LB at 37 °C (shaking at 220 rpm was added as a condition for liquid cultures). When necessary, 20 $\mu\text{g}/\text{mL}$ tetracycline was used for both *C. metallidurans* CH34 and *E. coli* strains (Tc^+ , Gen^+). Gentamycin at a concentration of 10 $\mu\text{g}/\text{mL}$ was used when growing *C. metallidurans* CH34 strains.

Plasmid Design and the Cloning Procedure. All of the plasmids used in this study are reported in Table S8. Oligonucleotide primers were synthesized by IDT DNA Technologies, and their sequences are reported in Table S9. The P_{pan} promoter was synthesized with no codon optimization by Genescript Biotech (Leiden, The Netherlands) and was delivered in the plasmid pUC57- P_{pan} .

A Q5 High-Fidelity 2X Master Mix (NEB) and a QuickLoad Taq 2X master mix were used for PCR amplification for cloning and colony PCR, respectively. An NEB Builder Hi-Fi DNA Assembly Master Mix (NEB) was used for the assembly of plasmid DNA after the plasmid design was carried out using the NEBuilder tool. A QIAprep Spin Miniprep Kit was used to isolate plasmid DNA (Qiagen). Restriction enzymes were purchased from NEB, and gel-purified DNA fragments were extracted with a Zymoclean Gel DNA Recovery Kit (Zymo Research) as per the manufacturer's recommendations. Plasmids were confirmed by Sanger sequencing (Eurofins). Details of plasmid construction are reported in the Supporting Information. Chemically competent *E. coli* DH5a and *E. coli* S17-1 were transformed via heat shock with the plasmid of interest.⁶⁰

Plasmid Delivery in *C. metallidurans* CH34. Bacterial conjugation was performed by growing overnight in liquid LB media. *C. metallidurans* CH34 and *E. coli* S17-1 were transformed with the desired plasmid. The following day, 1 mL of each culture was washed twice in PBS and eventually resuspended in 30 μL of PBS. The cultures were then mixed, placed on an LB-agar Petri dish (Starstedt), and incubated overnight at 30 °C. Plasmids pMTL74311- $\text{RBIC9}_{\Delta pyrE}$ and pMTL74311- $\text{RBIC9}_{\Delta pilAE}$ were delivered via conjugation. pMTL74311- $\text{RBIC9}_{\Delta pilE}$, pMTL74311- $\text{RBIC9}_{\Delta pilA}$, and pMTL74311- $\text{RBIC9}_{\Delta pilAE}::GFP$ were delivered via electro-

poration using a protocol described elsewhere for the preparation of the competent cells and electroporation.⁶¹ Plasmid pMTL74311- $\text{RBIC9}_{\Delta pilAE}::\lambda_{pr}GFP$ was delivered via both conjugation and electroporation.

Study of the Promoter and Riboswitch Libraries. *C. metallidurans* CH34 was electroporated with the plasmids for the riboswitch or constitutive promoter libraries. Cultures were resuspended to OD_{600} 0.05 in fresh LB media, and 200 μL was distributed in a black bottom 96-well plate (Thermo Scientific). The plates were incubated in a Cytomat 2C incubator at 30 °C, 800 rpm for 48 h, and were fed into a Molecular Devices SpectraMax i3 plate reader using a PreciseSCARA robotic arm OD_{600} . mRFP1 was excited at 585 nm, emission was detected at 620 nm, and OD measurement was done at 600 nm. mRFP1 levels (Arbitrary Units, au) at the end of the experiment were plotted for each plasmid construct for the constitutive promoter and riboswitch library. For the P_{BAD} -Riboswitch library, mRFP1 expression levels were studied in the presence of 5 mM theophylline and 0.1% L-arabinose (ON_ON) or in the presence of L-arabinose only (OFF_ON). Activation ratios were calculated as follows

$$P_{\text{BAD}} \text{ promoter library: activation ratio} = \frac{\text{mRFP1 au (+theophylline + arabinose)}}{\text{mRFP1 au (-theophylline + arabinose)}}$$

A study of the relative contribution of the P_{BAD} promoter and RBI to the expression of mRFP1 was performed without inducers (OFF_OFF), in the presence of only theophylline (Th_{OFF}), only arabinose (OFF_{Ar}), and both inducers (Th_{Ar})

Protocol for the Validation of the CRISPR-Cas9 System. To obtain knockouts of *C. metallidurans* CH34, the procedure was adapted and modified from the work of Cañadas and colleagues²¹ as follows.

Selection of Transformants and the Isolation of Mother Colonies. After 3–5 days of the delivery of the plasmid, transformants were selected on LB Tc^+ Gen^+ agar plates. Two colonies for each transformation event were streaked on LB Tc^+ Gen^+ agar plates to generate mother colonies with enough biomass for induction.

Induction of the Mother Colonies. A 1 μL loop was used to resuspend the mother colonies in 100 μL of PBS. These were then plated on LB induction agar plates (LB IND, supplemented with tetracycline, gentamycin, 5 mM theophylline, 0.1% L-arabinose) and incubated at 30 °C for 3–5 days.

Confirmation of Recombinant Isolates. Isolates growing on the LB induction agar plates were then streaked on LB Gen^+ agar plates and subjected to colony PCR with primer pair external to the homology arms and primer pairs with one primer external to the homology arms and the other primer inside the deleted genes.

Curing of CRISPR-Cas9 Plasmids. Recombinant clones were grown overnight in LB Gen^+ at 30 °C 200 rpm, serially diluted, plated on LB Gen^+ agar plates, and incubated at 30 °C for 24 h. Overall, 48 isolates were resuspended in 100 μL of PBS and replica plated on LB Tc^+ Gen^+ and LB Gen^+ to verify the plasmid loss. Finally, cPCR with primer pairs C9_cPCR_Fw/Rv amplifying Cas9 (Table S9) was performed to exclude the presence of the editing plasmid.

Storage of the Recombinant Isolates. cPCR was performed again on isolates that lost the plasmid (not growing on LB Tc^+

Gen⁺ agar plates). These were then grown overnight in LB Gen⁺ for the creation of cell banking.

To obtain the $\Delta pyrE$ knockouts, the following modifications were made to the protocol.

Selection of Transformants and the Isolation of Mother Colonies. Selection of transformants was performed on SGMM Tc⁺ Gen⁺ Ur⁺ agar plates.

Induction of the Mother Colonies. Induction of the mother colonies was performed on SGMM Tc⁺ Gen⁺ Ur⁺ Th⁺ Ar⁺ agar plates.

Confirmation of Recombinant Isolates. Confirmation of recombinant isolates was performed on SGMM Gen⁺ Ur⁺ agar plates.

Curing of CRISPR-Cas9 Plasmids. Recombinant clones were grown overnight in SGMM Gen⁺ Ur⁺ at 30 °C 200 rpm, serially diluted, plated on SGMM Gen⁺ Ur⁺ agar plates, and incubated at 30 °C for 24–48 h. Overall, 48 isolates were resuspended in 100 μ L of PBS and replica plated on SGMM Gen⁺ Tc⁺ Ur⁺ and SGMM Gen⁺ Ur⁺ to verify the plasmid loss.

Storage of the Recombinant Isolates. This was performed as for other recombinant strains, but the growth of isolates was done using SGMM Gen⁺ Ur⁺ liquid media.

Growth of the Biofilm of *C. metallidurans* sp. on SPCE. *C. metallidurans* CH34 was grown in 7.5 mL of SGMM in a 50 mL falcon tube, shaking at 220 rpm and 40 °C for 48 h. It was then washed twice in PBS and resuspended in PBS pH 6.9 at OD₆₀₀ 3.5. A total of 4 mL of the culture was placed into a 20 mL scintillation vial (Starstedt) and transferred into an anaerobic cabinet (Don Whitley Scientific). SPCE was washed with ddH₂O, sterilized with 70% ethanol, rinsed again in ddH₂O, transferred to the scintillation vial, and incubated for 24 h in AnO₂ conditions. After incubation, the electrode was gently rinsed with PBS pH 6.9 2% Na–gluconate. Then, 200 μ L of PBS pH 6.9 2% Na–gluconate was then placed so to cover the electrodes, and cyclic voltammetry experiments were finally performed.

Confocal Microscopy. *C. metallidurans* CH34, *C. metallidurans* CH34 $\Delta pilAE::GF$, and *C. metallidurans* CH34 $\Delta pilAE::\lambda_{pr}::GFP$ were grown as previously described. Bacterial cultures were normalized to OD₆₀₀ 0.5 and collected by centrifugation at 4000 rpm for 5 min. After two washes with PBS, cell membranes were stained with 5 mM FM 4-64 (ThermoFisher) dye in PBS for 30 min in the dark. After staining, cells were collected by centrifugation at 2000 rpm for 10 min, washed twice with PBS, and eventually resuspended in 100 mL of a Fluoromount-G water-based mounting medium (ThermoFisher). Overall, 5 μ L of a cell suspension was placed on an 18 mm borosilicate glass square coverslip (FisherScientific) and mounted on a frosted microscope slide (Thermo Scientific). Images were taken with a Zeiss Elyra Super Resolution Microscope using a Plan-Apochromat 63 \times /1.4 Oil DIC M27 objective. The structured illumination microscopy (SIM) mode was used with the following settings. Two tracks were set up for lasers 488 nm at 4 and 8% power and 100 and 200 ms exposure for GFP and FM 4-64, respectively. Super-resolution microscopy (SRM) and SIM grating periods were 28 and 42 nm for the green and red tracks, respectively, while bandpass filters employed were BP 495–550 + LP 750 for the green channel and LP 655 for the red channel. The channel shift was corrected using the Zen Channel Alignment Tool.

For live/dead staining of the SPCEs, after cyclic voltammetry experiments, the SPCE used for the study of electrophysiological properties of *C. metallidurans* CH34 was removed from AnO₂

conditions and stained for 30 min in the dark at RT with 5 mM Syto9 and 20 mM PI. After staining, the electrodes with the staining solution were placed in 35 mm Nunc Glass Bottom Dishes (ThermoFisher) and imaged using a Zeiss Elyra Super Resolution Microscope using a Plan-Apochromat 20 \times objective. The excitation of Syto9 and PI was performed with lasers 488 nm and 561 nm, while the detection was obtained in the windows of 499–570 and 588–685, respectively. The power of both lasers was set at 1%. The Z-stack was obtained by scanning 17 slices of 16 μ m each.

Cyclic Voltammetry. Zensor TE-100 SPCE was used for all of the electrochemical analysis. Initially, an electrode batch test ($n = 5$) was performed by covering WE, CE, and RE with 1 mM ferricyanide in AnO₂ conditions in an anaerobic cabinet (Don Whitley Scientific) with an mStat-i 400s portable potentiostat (Metrohm DropSens). The pretreatment of the electrodes was performed by repetitive cycling by performing CV between 0.6 and –0.6 V at 100 mV/s vs Ag/AgCl for 70 cycles.

Electrochemical experiments were all performed in AnO₂ conditions. *C. metallidurans* CH34 was grown for 48 h in 7.5 mL of SGMM in a 50 mL falcon tube, washed twice in PBS, and resuspended in PBS pH 6.9 at OD₆₀₀ 3.5. A total of 4 mL of the culture was placed in a 20 mL scintillation vial (Starstedt) and transferred into an AnO₂ cabinet (Don Whitley Scientific). CV measurements of biofilm-modified SPCEs were taken by performing CV between 0.6 and –0.6 V at 1, 5, or 20 mV/s vs Ag/AgCl. For scan rate studies, CV experiments were performed at 5, 10, 15, 20, 30, 50, and 100 mV/s vs Ag/AgCl. SPCE incubated in PBS pH 6.9 but with no cells was used as a negative control.

Dropview 8400 software (Metrohm DropSens) was used for recording voltammograms. A polynomial fitting baseline subtraction tool was used for the subtraction of the baseline from current peaks.

Bioinformatic and Statistical Analysis. The Uniprot Blast tool (<https://www.uniprot.org/blast>) was used to identify similar primary amino acid sequences of *G. sulfureducens* PilA (GSU1496) in the genome of *C. metallidurans* (strain ATCC 43123/DSM 2839/NBRC 102507/CH34). Clustal Omega (<https://www.ebi.ac.uk/Tools/msa/clustalo/>) was used to align the amino acid sequences between type IV pili of *G. sulfureducens* and *C. metallidurans* CH34. Illumina sequencing was provided by MicrobesNG (<https://microbesng.com>). CLC Genomic Workbench was used to analyze the whole-genome sequencing data. Program default parameters were used to analyze single nucleotide variants (SNVs), insertion and deletions (InDels), and structural variations (SVs).

■ ASSOCIATED CONTENT

SI Supporting Information

The Supporting Information is available free of charge at <https://pubs.acs.org/doi/10.1021/acssynbio.2c00130>.

Plasmid construction, (Figure S1) clustal alignment, (Figure S2) and (Table S3) colony PCR strategy, (Figure S4) transformation efficiencies of pMTL74311_P_{BAD}RBIC9_ $\Delta pilAE::\lambda GFP$, (Table S5) illumina sequencing of *C. metallidurans* CH34 knockouts, (Figure S6) confocal microscopy of biofilms, (Figure S7) scan rate experiment, (Table S8) plasmids and strains, (Table S9) oligonucleotide sequences, and (Table S10) spacer sequences (PDF)

AUTHOR INFORMATION

Corresponding Author

Katalin Kovacs – Division of Molecular Therapeutics and Formulations, School of Pharmacy, University of Nottingham, Nottingham NG7 2RD, United Kingdom; orcid.org/0000-0002-0622-940X; Email: Katalin.Kovacs@nottingham.ac.uk

Authors

Federico Turco – School of Pharmacy, Biodiscovery Institute, University of Nottingham, Nottingham NG7 2RD, United Kingdom

Marco Garavaglia – BBSRC/EPSC Synthetic Biology Research Centre, School of Life Sciences, Biodiscovery Institute, University of Nottingham, Nottingham NG7 2RD, United Kingdom

Rob Van Houdt – Microbiology Unit, Belgian Nuclear Research Centre (SCK CEN), 2400 Mol, Belgium; orcid.org/0000-0002-7459-496X

Phil Hill – School of Biosciences, The University of Nottingham, Leicestershire LE12 5RD, United Kingdom

Frankie J. Rawson – Bioelectronics Laboratory, School of Pharmacy, University of Nottingham, Nottingham NG7 2RD, United Kingdom; orcid.org/0000-0002-4872-8928

Complete contact information is available at:

<https://pubs.acs.org/10.1021/acssynbio.2c00130>

Author Contributions

Conceptualization was provided by F.T., M.G., F.J.R., P.H., and K.K.; methodology was given by F.T., M.G., and R.V.H.; investigation was performed by F.T. and M.G.; resources were provided by F.J.R., P.H., and K.K.; data curation was conducted by F.T., M.G., F.J.R., P.H., R.V.H., and K.K.; writing—original draft preparation was done by F.T., M.G., F.J.R., P.H., R.V.H., and K.K.; writing—review and editing was done by F.T., M.G., F.J.R., P.H., R.V.H., and K.K.; supervision was performed by M.G., F.J.R., P.H., R.V.H., and K.K.; and funding acquisition was done by F.J.R., P.H., and K.K. All authors have read and agreed to the published version of the manuscript.

Funding

This research was funded by the Biotechnology and Biological Sciences Research Council (BBSRC) (Grant Number BB/L013940/1) and the Engineering and Physical Sciences Research Council (EPSRC) under the same grant number. F.T. received the PhD studentship from the Biotechnology and Biological Sciences Research Council (Grant Number BB/M008770/1). F.J.R. received funding from the Engineering and Physical Sciences Research Council (EPSRC), Grant Number EP/R004072/1.

Notes

The authors declare no competing financial interest.

ABBREVIATIONS

cPCR, colony PCR; CDS, coding sequence; EET, extracellular electron transfer; MET, mediated electron transfer; MFC, microbial fuel cells; SD, Shine Dalgarno sequence; SIM, structural illumination microscopy; SPCE, screen-printed carbon electrodes

REFERENCES

(1) Van Houdt, R.; Monsieurs, P.; Mijndonckx, K.; Provoost, A.; Janssen, A.; Mergeay, M.; Leys, N. Variation in genomic islands

contribute to genome plasticity in *Cupriavidus metallidurans*. *BMC Genomics* **2012**, *13*, 111.

(2) Van Houdt, R.; Monchy, S.; Leys, N.; Mergeay, M. New mobile genetic elements in *Cupriavidus metallidurans* CH34, their possible roles and occurrence in other bacteria. *Antonie van Leeuwenhoek* **2009**, *96*, 205–226.

(3) Mergeay, M.; Nies, D.; Schlegel, H. G.; Gerits, J.; Charles, P.; Van Gijsegem, F. *Alcaligenes eutrophus* CH34 is a facultative chemolithotroph with plasmid-bound resistance to heavy metals. *J. Bacteriol.* **1985**, *162*, 328–334.

(4) Mijndonckx, K.; Provoost, A.; Monsieurs, P.; Leys, N.; Mergeay, M.; Mahillon, J.; Van Houdt, R. Insertion sequence elements in *Cupriavidus metallidurans* CH34: distribution and role in adaptation. *Plasmid* **2011**, *65*, 193–203.

(5) Reith, F.; Etschmann, B.; Grosse, C.; Moors, H.; Benotmane, M. A.; Monsieurs, P.; Grass, G.; Doonan, C.; Vogt, S.; Lai, B.; et al. Mechanisms of gold biomineralization in the bacterium *Cupriavidus metallidurans*. *Proc. Natl. Acad. Sci. U.S.A.* **2009**, *106*, 17757–17762.

(6) Ali, M. M.; Provoost, A.; Maertens, L.; Leys, N.; Monsieurs, P.; Charlier, D.; Van Houdt, R. Genomic and Transcriptomic Changes that Mediate Increased Platinum Resistance in *Cupriavidus metallidurans*. *Genes* **2019**, *10*, 63.

(7) Janssen, P. J.; Van Houdt, R.; Moors, H.; Monsieurs, P.; Morin, N.; Michaux, A.; Benotmane, M. A.; Leys, N.; Vallaey, T.; Lapidus, A.; et al. The complete genome sequence of *Cupriavidus metallidurans* strain CH34, a master survivalist in harsh and anthropogenic environments. *PLoS One* **2010**, *5*, No. e10433.

(8) Rogiers, T.; Merroun, M. L.; Williamson, A.; Leys, N.; Houdt, R. V.; Boon, N.; Mijndonckx, K. *Cupriavidus metallidurans* NA4 actively forms polyhydroxybutyrate-associated uranium-phosphate precipitates. *J. Hazard. Mater.* **2022**, *421*, No. 126737.

(9) Valls, M.; Atrian, S.; de Lorenzo, V.; Fernández, L. A. Engineering a mouse metallothionein on the cell surface of *Ralstonia eutropha* CH34 for immobilization of heavy metals in soil. *Nat. Biotechnol.* **2000**, *18*, 661–665.

(10) Biondo, R.; da Silva, F. A.; Vicente, E. J.; Souza Sarkis, J. E.; Schenberg, A. C. Synthetic phytochelatin surface display in *Cupriavidus metallidurans* CH34 for enhanced metals bioremediation. *Environ. Sci. Technol.* **2012**, *46*, 8325–8332.

(11) Wiesemann, N.; Mohr, J.; Grosse, C.; Herzberg, M.; Hause, G.; Reith, F.; Nies, D. H. Influence of copper resistance determinants on gold transformation by *Cupriavidus metallidurans* strain CH34. *J. Bacteriol.* **2013**, *195*, 2298–2308.

(12) Lambert, J. M.; Bongers, R. S.; Kleerebezem, M. Cre-lox-based system for multiple gene deletions and selectable-marker removal in *Lactobacillus plantarum*. *Appl. Environ. Microbiol.* **2007**, *73*, 1126–1135.

(13) Corts, A. D.; Thomason, L. C.; Gill, R. T.; Gralnick, J. A. A new recombinering system for precise genome-editing in *Shewanella oneidensis* strain MR-1 using single-stranded oligonucleotides. *Sci. Rep.* **2019**, *9*, No. 39.

(14) Vandecraen, J.; Chandler, M.; Aertsen, A.; Van Houdt, R. The impact of insertion sequences on bacterial genome plasticity and adaptability. *Crit. Rev. Microbiol.* **2017**, *43*, 709–730.

(15) Mougias, I.; Bosma, E. F.; Ganguly, J.; van der Oost, J.; van Kranenburg, R. Hijacking CRISPR-Cas for high-throughput bacterial metabolic engineering: advances and prospects. *Curr. Opin. Biotechnol.* **2018**, *50*, 146–157.

(16) Hsu, P. D.; Lander, E. S.; Zhang, F. Development and applications of CRISPR-Cas9 for genome engineering. *Cell* **2014**, *157*, 1262–1278.

(17) Li, N.; Wang, M.; Yu, S.; Zhou, J. Optimization of CRISPR-Cas9 through promoter replacement and efficient production of L-homoserine in *Corynebacterium glutamicum*. *Biotechnol. J.* **2021**, *16*, No. 2100093.

(18) Mougias, I.; Orsi, E.; Ghiffary, M. R.; Post, W.; de Maria, A.; Adiego-Perez, B.; Kengen, S. W. M.; Weusthuis, R. A.; van der Oost, J. Efficient Cas9-based genome editing of *Rhodobacter sphaeroides* for metabolic engineering. *Microb. Cell Fact.* **2019**, *18*, 204.

- (19) Tapscoff, T.; Guarnieri, M. T.; Henard, C. A. Development of a CRISPR/Cas9 System for *Methylococcus capsulatus* In Vivo Gene Editing. *Appl. Environ. Microbiol.* **2019**, *85*, No. e00340-19.
- (20) Xiong, B.; Li, Z.; Liu, L.; Zhao, D.; Zhang, X.; Bi, C. Genome editing of *Ralstonia eutropha* using an electroporation-based CRISPR-Cas9 technique. *Biotechnol. Biofuels* **2018**, *11*, 172.
- (21) Cañadas, I. C.; Groothuis, D.; Zygouropoulou, M.; Rodrigues, R.; Minton, N. P. RiboCas: A Universal CRISPR-Based Editing Tool for *Clostridium*. *ACS Synth. Biol.* **2019**, *8*, 1379–1390.
- (22) Tofalos, A. E.; Daghigho, M.; Gonzalez, M.; Papacchini, M.; Franzetti, A.; Seeger, M. Toluene degradation by *Cupriavidus metallidurans* CH34 in nitrate-reducing conditions and in Bioelectrochemical Systems. *FEMS Microbiol. Lett.* **2018**, *365*, No. fny119.
- (23) Walker, N. L.; Williams, A. P.; Styles, D. Pitfalls in international benchmarking of energy intensity across wastewater treatment utilities. *J. Environ. Manage.* **2021**, *300*, No. 113613.
- (24) Koffi, N. J.; Okabe, S. High voltage generation from wastewater by microbial fuel cells equipped with a newly designed low voltage booster multiplier (LVBM). *Sci. Rep.* **2020**, *10*, No. 18985.
- (25) Bird, L. J.; Kundu, B. B.; Tschirhart, T.; Cortis, A. D.; Su, L.; Gralnick, J. A.; Ajo-Franklin, C. M.; Glaven, S. M. Engineering Wired Life: Synthetic Biology for Electroactive Bacteria. *ACS Synth. Biol.* **2021**, *10*, 2808–2823.
- (26) von Canstein, H.; Ogawa, J.; Shimizu, S.; Lloyd, J. R. Secretion of Flavins by *Shewanella* Species and Their Role in Extracellular Electron Transfer. *Appl. Environ. Microbiol.* **2008**, *74*, 615–623.
- (27) Reguera, G.; McCarthy, K. D.; Mehta, T.; Nicoll, J. S.; Tuominen, M. T.; Lovley, D. R. Extracellular electron transfer via microbial nanowires. *Nature* **2005**, *435*, 1098–1101.
- (28) Richter, L. V.; Sandler, S. J.; Weis, R. M. Two isoforms of *Geobacter sulfurreducens* PilA have distinct roles in pilus biogenesis, cytochrome localization, extracellular electron transfer, and biofilm formation. *J. Bacteriol.* **2012**, *194*, 2551–2563.
- (29) Reguera, G.; Nevin, K. P.; Nicoll, J. S.; Covalla, S. F.; Woodard, T. L.; Lovley, D. R. Biofilm and nanowire production leads to increased current in *Geobacter sulfurreducens* fuel cells. *Appl. Environ. Microbiol.* **2006**, *72*, 7345–7348.
- (30) Lovley, D. R.; Yao, J. Intrinsically Conductive Microbial Nanowires for “Green” Electronics with Novel Functions. *Trends Biotechnol.* **2021**, *39*, 940–952.
- (31) Fairbrother, L.; Etschmann, B.; Brugger, J.; Shapter, J.; Southam, G.; Reith, F. Biomineralization of gold in biofilms of *Cupriavidus metallidurans*. *Environ. Sci. Technol.* **2013**, *47*, 2628–2635.
- (32) Topp, S.; Reynoso, C. M. K.; Seeliger, J. C.; Goldust, I. S.; Desai, S. K.; Murat, D.; Shen, A.; Puri, A. W.; Komeili, A.; Bertozzi, C. R.; et al. Synthetic Riboswitches That Induce Gene Expression in Diverse Bacterial Species. *Appl. Environ. Microbiol.* **2010**, *76*, 7881–7884.
- (33) Schumann, K.; Lin, S.; Boyer, E.; Simeonov, D. R.; Subramaniam, M.; Gate, R. E.; Haliburton, G. E.; Ye, C. J.; Bluestone, J. A.; Doudna, J. A.; Marson, A. Generation of knock-in primary human T cells using Cas9 ribonucleoproteins. *Proc. Natl. Acad. Sci. U.S.A.* **2015**, *112*, 10437–10442.
- (34) Siegele, D. A.; Hu, J. C. Gene expression from plasmids containing the araBAD promoter at subsaturating inducer concentrations represents mixed populations. *Proc. Natl. Acad. Sci. U.S.A.* **1997**, *94*, 8168–8172.
- (35) Ribeiro-dos-Santos, G.; Biondo, R.; Quadros Ode, F.; Vicente, E. J.; Schenberg, A. C. A metal-repressed promoter from gram-positive *Bacillus subtilis* is highly active and metal-induced in gram-negative *Cupriavidus metallidurans*. *Biotechnol. Bioeng.* **2010**, *107*, 469–477.
- (36) Kincade, J. M.; deHaseth, P. L. Bacteriophage lambda promoters pL and pR sequence determinants of in vivo activity and of sensitivity to the DNA gyrase inhibitor, coumermycin. *Gene* **1991**, *97*, 7–12.
- (37) Van Houdt, R.; Provoost, A.; Van Assche, A.; Leys, N.; Lievens, B.; Mijndendonckx, K.; Monsieurs, P. *Cupriavidus metallidurans* Strains with Different Mobilomes and from Distinct Environments Have Comparable Phenomes. *Genes* **2018**, *9*, 507.
- (38) Arikawa, H.; Matsumoto, K. Evaluation of gene expression cassettes and production of poly (3-hydroxybutyrate-co-3-hydroxyhexanoate) with a fine modulated monomer composition by using it in *Cupriavidus necator*. *Microb. Cell Fact.* **2016**, *15*, 184.
- (39) Vidal, L.; Pinsach, J.; Striedner, G.; Caminal, G.; Ferrer, P. Development of an antibiotic-free plasmid selection system based on glycine auxotrophy for recombinant protein overproduction in *Escherichia coli*. *J. Biotechnol.* **2008**, *134*, 127–136.
- (40) Tegel, H.; Ottosson, J.; Hober, S. Enhancing the protein production levels in *Escherichia coli* with a strong promoter. *FEBS J.* **2011**, *278*, 729–739.
- (41) Kato, Y. Extremely Low Leakage Expression Systems Using Dual Transcriptional-Translational Control for Toxic Protein Production. *Int. J. Mol. Sci.* **2020**, *21*, 705.
- (42) Ehsaan, M.; Baker, J.; Kovács, K.; Malys, N.; Minton, N. P. The pMTL70000 modular, plasmid vector series for strain engineering in *Cupriavidus necator* H16. *J. Microbiol. Methods* **2021**, *189*, No. 106323.
- (43) Bi, C.; Su, P.; Muller, J.; Yeh, Y. C.; Chhabra, S. R.; Beller, H. R.; Singer, S. W.; Hillson, N. J. Development of a broad-host synthetic biology toolbox for *Ralstonia eutropha* and its application to engineering hydrocarbon biofuel production. *Microb. Cell Fact.* **2013**, *12*, 107.
- (44) Volke, D. C.; Friis, L.; Wirth, N. T.; Turlin, J.; Nickel, P. I. Synthetic control of plasmid replication enables target-and self-curing of vectors and expedites genome engineering of *Pseudomonas putida*. *Metab. Eng. Commun.* **2020**, *10*, No. e00126.
- (45) Srinivas, S.; Hu, Z.; Cronan, J. E. *Escherichia coli* vectors having stringently repressible replication origins allow a streamlining of Crispr/Cas9 gene editing. *Plasmid* **2019**, *103*, 53–62.
- (46) Deatherage, D. E.; Leon, D.; Rodriguez, A. E.; Omar, S. K.; Barrick, J. E. Directed evolution of *Escherichia coli* with lower-than-natural plasmid mutation rates. *Nucleic Acids Res.* **2018**, *46*, 9236–9250.
- (47) Nevin, K. P.; Kim, B. C.; Glaven, R. H.; Johnson, J. P.; Woodard, T. L.; Methe, B. A.; DiDonato, R. J.; Didonato, R. J.; Covalla, S. F.; Franks, A. E.; Liu, A. Anode biofilm transcriptomics reveals outer surface components essential for high density current production in *Geobacter sulfurreducens* fuel cells. *PLoS One* **2009**, *4*, No. e5628.
- (48) Baharoglu, Z.; Bikard, D.; Mazel, D. Conjugative DNA transfer induces the bacterial SOS response and promotes antibiotic resistance development through integron activation. *PLoS Genet.* **2010**, *6*, No. e1001165.
- (49) Millacura, F. A.; Janssen, P. J.; Monsieurs, P.; Janssen, A.; Provoost, A.; Van Houdt, R.; Rojas, L. A. Unintentional Genomic Changes Endow *Cupriavidus metallidurans* with an Augmented Heavy-Metal Resistance. *Genes* **2018**, *9*, 551.
- (50) Kilmury, S. L. N.; Burrows, L. L. Type IV pilins regulate their own expression via direct intramembrane interactions with the sensor kinase PilS. *Proc. Natl. Acad. Sci. U.S.A.* **2016**, *113*, 6017–6022.
- (51) Aoki, K. J.; Chen, J.; Liu, Y.; Jia, B. Peak potential shift of fast cyclic voltammograms owing to capacitance of redox reactions. *J. Electroanal. Chem.* **2020**, *856*, No. 113609.
- (52) Elgrishi, N.; Rountree, K. J.; McCarthy, B. D.; Rountree, E. S.; Eisenhart, T. T.; Dempsey, J. L. A practical beginner’s guide to cyclic voltammetry. *J. Chem. Educ.* **2018**, *95*, 197–206.
- (53) Richter, H.; Nevin, K. P.; Jia, H.; Lowy, D. A.; Lovley, D. R.; Tender, L. M. Cyclic voltammetry of biofilms of wild type and mutant *Geobacter sulfurreducens* on fuel cell anodes indicates possible roles of OmcB, OmcZ, type IV pili, and protons in extracellular electron transfer. *Energy Environ. Sci.* **2009**, *2*, 506–516.
- (54) Gregg, B. A.; Heller, A. Redox polymer films containing enzymes. 2. Glucose oxidase containing enzyme electrodes. *J. Phys. Chem. A* **1991**, *95*, 5976–5980.
- (55) Schuetz, B.; Schicklberger, M.; Kuermann, J.; Spormann, A. M.; Gescher, J. Periplasmic electron transfer via the c-type cytochromes MtrA and FccA of *Shewanella oneidensis* MR-1. *Appl. Environ. Microbiol.* **2009**, *75*, 7789–7796.
- (56) Belchik, S. M.; Kennedy, D. W.; Dohnalkova, A. C.; Wang, Y.; Sevinc, P. C.; Wu, H.; Lin, Y.; Lu, H. P.; Fredrickson, J. K.; Shi, L. Extracellular reduction of hexavalent chromium by cytochromes MtrC and OmcA of *Shewanella oneidensis* MR-1. *Appl. Environ. Microbiol.* **2011**, *77*, 4035–4041.

(57) Marsili, E.; Baron, D. B.; Shikhare, I. D.; Coursolle, D.; Gralnick, J. A.; Bond, D. R. *Shewanella* secretes flavins that mediate extracellular electron transfer. *Proc. Natl. Acad. Sci. U.S.A.* **2008**, *105*, 3968–3973.

(58) Uriá, N.; Muñoz Berbel, X.; Sanchez, O.; Muñoz, F. X.; Mas, J. Transient storage of electrical charge in biofilms of *Shewanella oneidensis* MR-1 growing in a microbial fuel cell. *Environ. Sci. Technol.* **2011**, *45*, 10250–10256.

(59) Busalmen, J. P.; Esteve-Nunez, A.; Berna, A.; Feliu, J. M. C-type cytochromes wire electricity-producing bacteria to electrodes. *Angew. Chem., Int. Ed.* **2008**, *47*, 4874–4877.

(60) Chung, C. T.; Niemela, S. L.; Miller, R. H. One-step preparation of competent *Escherichia coli*: transformation and storage of bacterial cells in the same solution. *Proc. Natl. Acad. Sci. U.S.A.* **1989**, *86*, 2172–2175.

(61) Choi, K. H.; Kumar, A.; Schweizer, H. P. A 10-min method for preparation of highly electrocompetent *Pseudomonas aeruginosa* cells: application for DNA fragment transfer between chromosomes and plasmid transformation. *J. Microbiol. Methods* **2006**, *64*, 391–397.

Recommended by ACS

Using the Strategy of Inducing and Genetically Transforming Plant Suspension Cells to Produce High Value-Added Bioactive Substances

Qian Li, Pengda Ma, *et al.*

JANUARY 12, 2022
JOURNAL OF AGRICULTURAL AND FOOD CHEMISTRY

READ [↗](#)

FMC to acquire BioPhero

Matt Blois.

JULY 18, 2022
C&EN GLOBAL ENTERPRISE

READ [↗](#)

A Self-Sustained System Spanning the Primary and Secondary Metabolism Stages to Boost the Productivity of *Streptomyces*

Ming Zhao, Dongzhi Wei, *et al.*

DECEMBER 24, 2021
ACS SYNTHETIC BIOLOGY

READ [↗](#)

Sarah Richardson

Cici Zhang.

MARCH 09, 2020
C&EN GLOBAL ENTERPRISE

READ [↗](#)

[Get More Suggestions >](#)